

# Graphene-Assisted Epitaxy of Nitrogen Lattice Polarity GaN Films on Non-Polar Sapphire Substrates for Green Light Emitting Diodes


Fang Liu, Zhihong Zhang, Xin Rong, Ye Yu, Tao Wang, Bowen Sheng, Jiaqi Wei, Siyuan Zhou, Xuelin Yang, Fujun Xu, Zhixin Qin, Yuantao Zhang,\* Kaihui Liu,\* Bo Shen, and Xinqiang Wang\*

Lattice polarity is a key point for hexagonal semiconductors such as GaN. Unfortunately, only Ga-polarity GaN have been achieved on graphene till now. Here, the epitaxy of high quality nitrogen-polarity GaN films on transferred graphene on non-polar sapphire substrates by molecular beam epitaxy is reported. This success is achieved through atomic nitrogen irradiation, where C–N bonds are formed in graphene and provide nucleation sites for GaN and leading to N-polarity GaN epitaxy. The N-polarity characteristics are confirmed by chemical etching and transmission electron microscopy measurement. Due to the higher growth temperature of InGaN at N-polarity than that at Ga-polarity, green light emitting diodes are fabricated on the graphene-assisted substrate, where a large redshift of emission wavelength is observed. These results open a new avenue for the polarity modulation of III-nitride films based on 2D materials, and also pave the way for potential application in longer wavelength light emitting devices.

Dr. F. Liu, Dr. Z. Zhang, Dr. X. Rong, Dr. T. Wang, Dr. B. Sheng, Dr. J. Wei, Dr. S. Zhou, Dr. X. Yang, Dr. F. Xu, Prof. Z. Qin, Prof. K. Liu, Prof. B. Shen, Prof. X. Wang  
State Key Laboratory for Mesoscopic Physics and Frontiers Science Center for Nano-optoelectronics School of Physics  
Peking University  
Beijing 100871, P. R. China  
E-mail: khliu@pku.edu.cn; wangshi@pku.edu.cn

Dr. Y. Yu, Prof. Y. Zhang  
State Key Laboratory of Integrated Optoelectronics  
College of Electronic Science and Engineering  
Jilin University  
Changchun 130012, P. R. China  
E-mail: zhangyt@jlu.edu.cn

Dr. T. Wang  
Electron Microscopy Laboratory  
School of Physics  
Peking University  
Beijing 00871, P. R. China  
Prof. K. Liu, Prof. B. Shen, Prof. X. Wang  
Collaborative Innovation Center of Quantum Matter  
Beijing 100871, P. R. China

 The ORCID identification number(s) for the author(s) of this article can be found under <https://doi.org/10.1002/adfm.202001283>.

DOI: 10.1002/adfm.202001283

## 1. Introduction

In recent years, quasi-van der Waals epitaxy (quasi-vdWE) of  $sp^3$ -hybridized III-nitride semiconductors on  $sp^2$ -hybridized 2D layered materials has attracted much interests.<sup>[1–4]</sup> For example, combining graphene and III-nitride semiconductors has led to some new kinds of light emitting devices and flexible optoelectronic devices.<sup>[5–9]</sup> In addition, the intermolecular dispersion interaction from graphene can largely relieve the stress between the substrate and the epilayer, leading to the epitaxy growth of strain-relaxed III-nitride materials.<sup>[10,11]</sup> Furthermore, it allows the transfer of epitaxial structures easily and eliminates the residual strain in the structures when they are released from the hetero-substrates.<sup>[12–14]</sup> Till now, most efforts of III-nitrides epitaxy are

based on metal organic vapor phase epitaxy (MOVPE), where an AlN nucleation/buffer layer is necessary to guarantee the successful epitaxy of GaN.<sup>[15–18]</sup> Oxygen-plasma pretreatment on the graphene is often used as a way to generate more nucleation sites for AlN.<sup>[19–22]</sup> In addition, GaN grown by MOVPE with oxygen-plasma pretreatment are all Ga-lattice-polarity while N-lattice-polarity has never been reported until now to the best of our knowledge.<sup>[23–29]</sup> In contrast to Ga-polarity GaN, N-polarity one offers a different atomic configuration in chemical activity, which not only allows the access to kinetic space in epitaxy that is not normally attainable on Ga-polarity surface, but also enables the fabrication of a variety of novel device structures.<sup>[30,31]</sup> Furthermore, since N-polarity InGaN, which acts as quantum well in the case of visible light emitting devices, stands higher growth temperature than Ga-polarity one and thus the In composition can be higher at the same growth temperature. This definitely benefits fabrication of nitrides-based light emitting diodes in longer wavelength, for example, green light.<sup>[32,33]</sup>

In this work, we successfully grow GaN films directly on graphene/sapphire substrate by using molecular beam epitaxy (MBE) without using AlN buffer layer. An atomic nitrogen irradiation is performed on the graphene, which generates N–C bonds. These N–C bonds not only provide feasibility for GaN

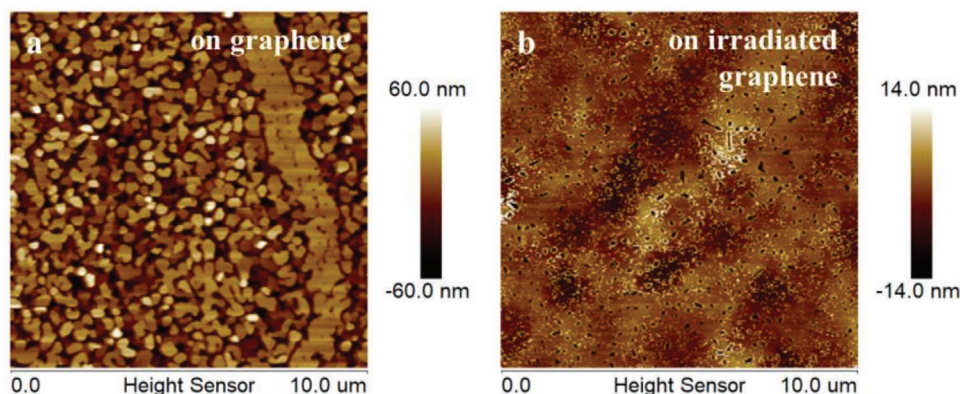


**Figure 1.** AFM images of 800 nm-thick GaN films grown on a) graphene/ $\text{Al}_2\text{O}_3$  and on b) atomic nitrogen irradiated graphene/ $\text{Al}_2\text{O}_3$ . The former shows a grain-like morphology, and the latter owes a drastically improved surface due to the improvement of GaN nucleation by atomic nitrogen irradiation of graphene.

nucleation but also lead to the N-lattice-polarity of the following grown GaN, as further confirmed by chemical etching and transmission electron microscopy measurement. The subsequent growth by MOVPE follows the N-lattice-polarity, which makes it easy to obtain the high In-composition InGaN and thus to fabricate the N-polarity nitrides-based green LEDs on graphene/sapphire for the first time.

## 2. Results and Discussion

### 2.1. Epitaxy of N-Polarity GaN Films on Atomic Nitrogen Irradiated Graphene

Monolayer graphene was grown on annealed (111)Cu substrate by chemical vapor deposition (CVD), and then was transferred onto a 2 in. c-plane  $\text{Al}_2\text{O}_3$  substrate.<sup>[34]</sup> Epitaxial growth of GaN films was performed on these graphene-coated  $\text{Al}_2\text{O}_3$  substrates using a plasma assisted MBE system. By nature, it is very difficult to grow GaN on graphene because there are no dangling bonds waiting for Ga or N to nucleate and form covalent bonds on the graphene surface. Therefore, Ga or N adatoms have to find some defect places where the 2D graphene is not perfect and thus can supply dangling bonds. This leads to a well-known problem that GaN tends to nucleate along the wrinkles of graphene, which are often observed in the transferred graphene on substrates without perfect bonding with graphene. This nucleation tendency often results in poor surface morphology of GaN, as shown in **Figure 1a**, a grain-like morphology is typically observed with a wide string area because of the nucleation along the wrinkles of graphene. The surface is quite rough with a root mean square (rms) roughness of 14.6 nm in a scanned area of  $10 \times 10 \mu\text{m}^2$ .

To solve this problem, we proposed to use an in-situ atomic nitrogen irradiation on the transferred graphene to generate more nucleation sites for GaN and thus to make GaN smoother. This atomic nitrogen is supplied by a N-plasma cell with a forward power of 350 W and a purified  $\text{N}_2$  gas with a flow rate of 0.8 standard cubic centimeters per minute (sccm). As shown in **Figure 1b**, surface flatness is drastically improved, where the rms value is as small as 3.4 nm in a scanned area of  $10 \times 10$

$\mu\text{m}^2$ . Although there are still a lot of pits on the surface, which is most likely due to some contamination during the graphene transfer process, the grain morphology has been completely suppressed, and high-quality 2D growth is achieved.

Checking the growth process, we did not find any difference between the growth behaviors of GaN on graphene with and without atomic nitrogen irradiation, as in-situ investigation by reflection high energy electron diffraction (RHEED). As shown in **Figure 2a**, before GaN epitaxy, RHEED patterns for graphene are clearly observed, though a little dim since that the graphene is only monolayer-thick and the transferred graphene on  $\text{Al}_2\text{O}_3$  substrate is slightly contaminated. This streaky pattern also tells us that the in-plane hexagonal arrangement of C atoms in graphene and that the surface is basically flat. This streak pattern did not show clear change under atomic nitrogen irradiation, implying that the lattice was kept. It is found that conventional low temperature growth of GaN buffer layer is not favorable for growth on graphene since the RHEED patterns of GaN nucleation layer at low temperature (LT) of 500 °C include single-crystal streaks and poly-crystal rings at the same azimuth (see **Figure S1**, Supporting Information). On the other hand, direct high temperature (HT) growth at 780 °C shows streaky patterns depicted in **Figure 2b**, displaying the single crystalline nucleation layer, thus leading to better crystalline quality of subsequent GaN epilayers. Therefore, we directly grew GaN layer at 780 °C without using LT-GaN buffer layer. Of course, those GaN layers are all grown under Ga-rich condition to improve the crystalline quality, where the Ga/N flux ratio is known as a key parameter for the growth (see **Figure S5**, Supporting Information). **Figure 2c** shows the RHEED patterns of grown GaN after cooling down to 550 °C, where  $(3 \times 3)$  surface reconstruction is clearly observed, indicating that the grown GaN is N-polarity.<sup>[35]</sup> This is different from that of GaN grown on the sapphire substrate without graphene, where no surface reconstruction can be observed and the GaN film is usually mixed polarities or mostly Ga-polarity, since no nitridation of sapphire was performed.

To further confirm the lattice polarity, scanning transmission electron microscopy (STEM) and chemical etching experiments were performed. **Figure 2d** shows cross-sectional atomically resolved annular bright-field (ABF) STEM image. It can be seen that a sharp interface between GaN and graphene is

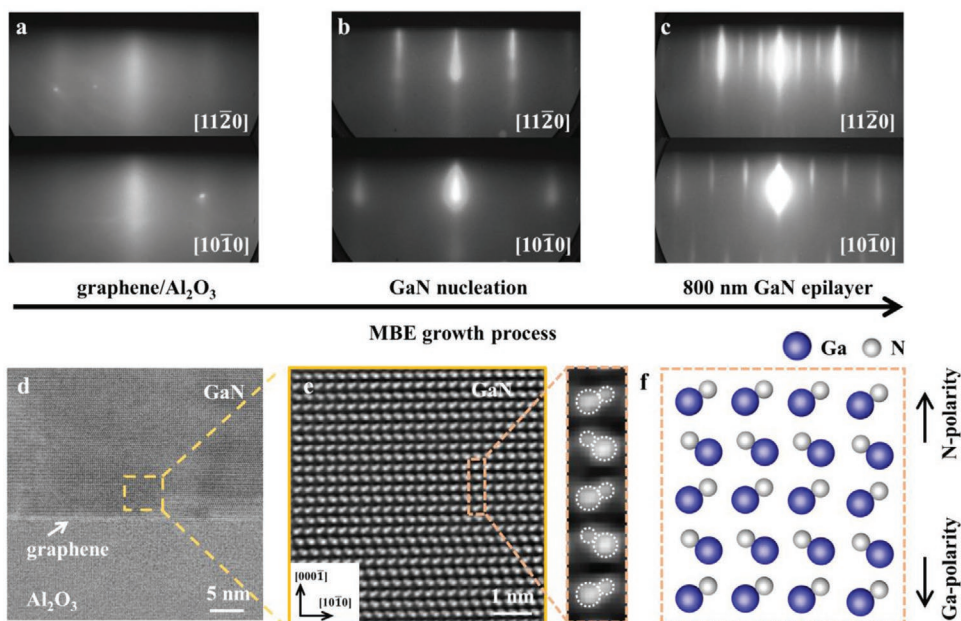


**Figure 2.** In situ RHEED images of GaN films grown on graphene/ $\text{Al}_2\text{O}_3$  substrates: a) initial graphene before epitaxy, b) high temperature GaN nucleation at  $780^\circ\text{C}$  and c) 800 nm-thick GaN epilayer cooling to  $550^\circ\text{C}$ . d) ABF-STEM image of GaN/graphene/ $\text{Al}_2\text{O}_3$  interface. e) iDPC-STEM image of GaN grown on atomic nitrogen irradiated graphene/ $\text{Al}_2\text{O}_3$  labeled by the frame in d), and f) the atomic model of N-polarity GaN. It is clear that the atomic arrangement of Ga and N atoms are exactly the same as that atomic model shown, confirmed the N-polarity for the grown GaN.

observed, where graphene exhibits a faint contrast between GaN and sapphire substrate. Figure 2e shows the integrated differential phase contrast (iDPC) STEM image of the zoom-in of Figure 2d, where Ga and N atoms can be clearly distinguished and the array of Ga and N atoms indicates the successful epitaxy of N-polarity GaN, as shown in Figure 2f, agreed with the RHEED patterns. In addition, we performed chemical etching on the GaN film. The GaN film was easily etched by KOH solution and the etched surface exhibited randomly distributed hexagonal pyramids, which are the same etching behavior as the N-polarity GaN (see Figure S2, Supporting Information).<sup>[36,37]</sup> Therefore, the chemical etching results also confirm the N-polarity for the GaN grown on graphene.

## 2.2. Atomic Model for Achieving N-Lattice-Polarity

Since there is only as-grown GaN on the graphene, the lattice polarity of GaN should be determined by the interface atomic bonding between GaN and graphene. To clarify the reason for formation of N-polarity GaN, X-ray photoelectron spectroscopy (XPS) was performed on graphene and atomic nitrogen irradiated graphene. As shown in Figure 3a, the N 1s peak at binding energy of  $\approx 400$  eV is clearly observed after the atomic nitrogen irradiation, indicating formation of N-related bonds. Figure 3b shows the zoom-in spectrum of the N 1s peak, which consists of two different types of C–N configurations, that is,  $\text{sp}^2$ -like C–N and  $\text{sp}^3$ -like C–N. There is no dangling bond

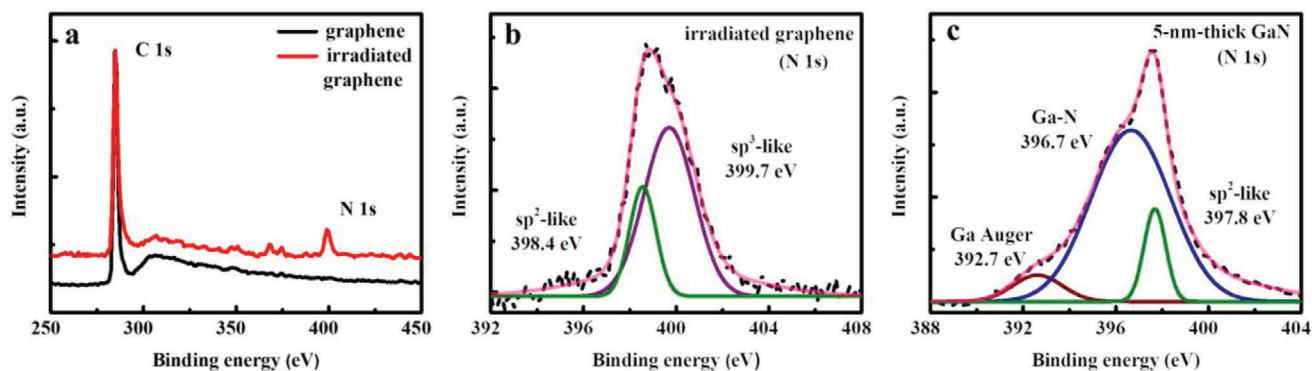


**Figure 3.** a) XPS survey spectra of graphene/ $\text{Al}_2\text{O}_3$  without and with atomic nitrogen irradiation. b) N 1s characteristic peak of the atomic nitrogen irradiated graphene/ $\text{Al}_2\text{O}_3$  substrate. It is shown that the N 1s peak includes a contribution from peaks of  $\text{sp}^3$ -like C–N bond (399.7 eV) and  $\text{sp}^2$ -like C–N bond (398.4 eV). The dominant contribution comes from the  $\text{sp}^3$ -like C–N bonds. c) N 1s characteristic peak of 5 nm-thick GaN nucleation on the atomic nitrogen irradiated graphene/ $\text{Al}_2\text{O}_3$  substrate. The N 1s peak consists of Ga–N bond (396.7 eV),  $\text{sp}^2$ -like C–N bond (397.8 eV) and Ga Auger signal (392.7 eV), showing the nucleation of  $\text{sp}^3$ -bonded GaN on  $\text{sp}^3$ -like C–N bonds.

for N atom in  $sp^2$ -like C–N bond, while there is one dangling bond left for each N atom in  $sp^3$ -like C–N bonds, as reported previously.<sup>[9,17,38]</sup> Therefore, when the Ga and N adatoms are supplied, Ga adatom will connect with this dangling bond to form C–N–Ga bond and thus initiate the growth. XPS study of 5-nm-thick GaN deposited on the graphene/ $Al_2O_3$  at 780 °C also confirms this. As shown in Figure 3c, broaden N 1s peak from Ga–N bonds confirms the epitaxy of  $sp^3$ -hybridized GaN on graphene. The  $sp^2$ -like C–N bond's peak maintains similar shape and full width at half maximum (FWHM) value while the  $sp^3$ -like C–N bond's peak disappears. This confirms that the GaN nucleates from the  $sp^3$ -like C–N bonds and thus the GaN is grown on top of them and prevents the penetration of X-ray. At the same time, the Ga Auger peak is also observed, which origins from the Ga-rich growth condition. Now, the interface structure between GaN and graphene and the initial nucleation of GaN on atomic nitrogen irradiated graphene is clarified.

As shown schematically in Figure 4a, graphene is firstly transferred to the sapphire substrate. During atomic nitrogen irradiation, C–N bonds have been formed, either  $sp^3$ -like C–N bonds or  $sp^2$ -like C–N bonds, as depicted in Figure 4b. Between them, the  $sp^2$ -like C–N bonds are inert for coming Ga adatoms since there is no dangling bond available. Ga adatoms will bond with  $sp^3$ -like C–N bonds to form C–N–Ga bonds. Then, along the growth direction, three N atoms will bond with each Ga atom to form C–N–Ga–N(3) structure, leading to the formation of N-polarity GaN, as shown in Figure 4c and Figure 4d. Note that the atomic nitrogen irradiation is the key point to control the lattice polarity and generate more nucleation sites so that the crystalline quality of GaN can be improved. Figure 5 shows the X-ray diffraction (XRD)  $\omega$ -rocking curves for (0002) and (10 $\bar{1}2$ ) planes of 800 nm-thick GaN layer grown on graphene with and without atomic nitrogen irradiation. It is clear that the FWHMs of  $\omega$ -rocking curves for (0002) and (10 $\bar{1}2$ ) planes decreases from 0.4° and 0.46° to 0.20° and 0.27° respectively, indicating improved crystalline quality. This

also coincides with the estimated dislocation density in GaN epilayers through TEM measurement (see Figure S7, Supporting Information).

### 2.3. Fabrication of N-Polarity Green InGaN-Based LEDs via Irradiated Graphene

We then grew an InGaN-based green LED structure on MBE-grown N-polarity GaN/graphene/ $Al_2O_3$  template by MOVPE. It was found that the lattice polarity was followed for the MOVPE-grown GaN, that is, N-polarity. As shown in Figure 6a, the LED structure consists of a Si-doped GaN layer, 5-period InGaN/GaN multiple-quantum-wells (MQWs), a p-type AlGaIn electron blocking layer (EBL) and Mg-doped hole-injection p-GaN/p<sup>+</sup>-GaN layers, respectively. Figure 6b shows the low temperature photoluminescence spectra for the LEDs on GaN grown with and without graphene, while other growth process stays exactly the same. It is observed that the emission peak redshifts from 462 to 537 nm, most likely because that the GaN on graphene is N-polarity, where the In composition of InGaN quantum wells is higher than that in the Ga-polarity case as we explained above. Furthermore, internal quantum efficiency (IQE) of those LEDs have been investigated by temperature-dependent PL measurement, where the IQE of LED structure with atomic nitrogen irradiated graphene is about 14% that is higher than  $\approx$ 3% for the structure without graphene (see Figure S8a,b, Supporting Information). It should be noted that growth of N-polarity GaN is actually rather difficult and the performance of N-polarity LED is inferior, in particular in green regime. We actually did a lot of work on fabrication of N-polarity green LED on C-face SiC substrates, an expensive substrate but with small lattice mismatch with GaN, where the IQE is about 10% (see Figure S8c, Supporting Information). Therefore, the  $\approx$ 14% of IQE for the N-polarity green LEDs on atomic nitrogen irradiated graphene definitely indicates the irradiated graphene improves

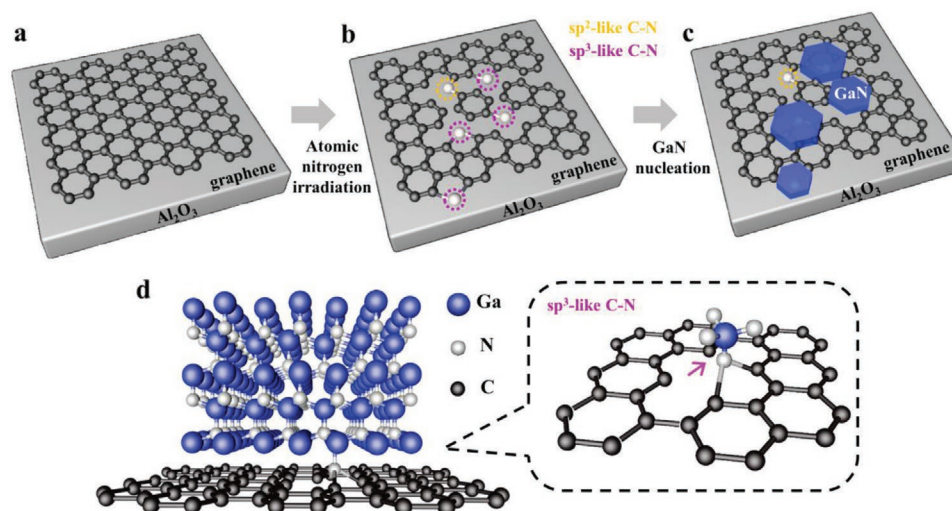


**Figure 4.** Schematic diagram of the nucleation growth of GaN on atomic nitrogen irradiated graphene/ $Al_2O_3$ : a) as-transferred graphene/ $Al_2O_3$ ; b) atomic nitrogen irradiated graphene/ $Al_2O_3$  with  $sp^2$ -like C–N bonds and  $sp^3$ -like C–N bonds, where the red ones indicate the  $sp^2$ -like C–N bond and the yellow ones show the  $sp^3$ -like C–N bond; c) GaN nucleation on graphene assisted by  $sp^3$ -like C–N bonds. d) Atomic structures of GaN on atomic nitrogen irradiated graphene via the C–N–Ga–N(3) bonding structure, which leads to the formation of N-polarity of subsequent GaN.

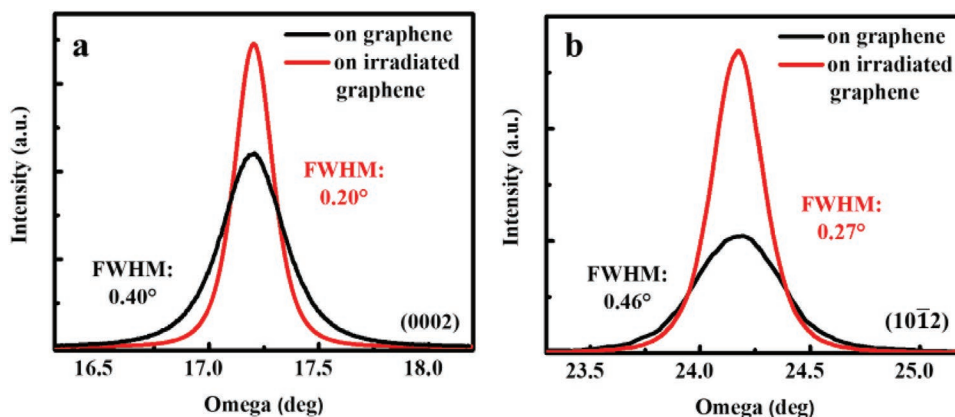


**Figure 5.** a,b) FWHMs of (0002)- and (10 $\bar{1}2$ )-plane XRCs for 800 nm-thick GaN films grown on graphene/Al<sub>2</sub>O<sub>3</sub> with or without atomic nitrogen irradiation. These reveal the crystalline quality improvement of GaN epilayers on irradiated graphene by improving GaN nucleation.

the crystalline quality of GaN layer. By the way, the emission from p-type GaN and the bottom n-type GaN are observed for both cases, which indicates that the p-type doping of GaN in the case of N-polarity is well achieved. As shown in Figure 6c, strong green emission is observed for the LEDs under electrical driving. This result thus provides a potential way to develop novel N-polarity LED structures with longer wavelengths.

### 3. Conclusion

In conclusion, we have achieved N-polarity GaN films on graphene/sapphire. It is found that atomic nitrogen irradiation leads to generation of sp<sup>3</sup>-like C–N bonds, which act as nucleation sites for the following GaN growth. This atomic nitrogen irradiation not only improves crystalline quality of GaN but also results in the growth of N-polarity of GaN. The reason of N-polarity is that each of N atom among those sp<sup>3</sup>-like C–N bonds provides single bond for the Ga adatoms and each bonded Ga atom bonds with three N atoms along the growth direction. The N-polarity is followed during the growth of green LEDs structure by MOVPE on top of GaN/graphene where a large emission redshift was observed due to the fact that the In incorporation capability is higher during the growth of InGaN quantum wells for the N-polarity than that for Ga-polarity. This

work opens a new avenue for the polarity control of III-nitride semiconductors based on 2D materials, and also paves the way for potential application in longer wavelength light emitting devices.

### 4. Experimental Section

**Graphene Growth and Transfer:** The polycrystalline Cu foil (25 μm-thick, 99.8%, Sichuan Oriental Stars Trading Co. Ltd., #Cu-1031) placed on a quartz substrate was loaded into the CVD furnace. The system was heated to 1020 °C in 1 h with 500 sccm Ar and kept at 1020 °C for 30 min to transform the Cu foil into single-crystal Cu(111). Then H<sub>2</sub> and CH<sub>4</sub> were introduced into the system to grow monolayer graphene. The annealing and graphene growth were conducted under atmosphere condition. The graphene was transferred onto Al<sub>2</sub>O<sub>3</sub> substrate by a PMMA-mediated wet transfer method. Graphene film was spin-coated with PMMA and baked at 120 °C for 2 min, and then the Cu was removed by 4% (NH<sub>4</sub>)<sub>2</sub>S<sub>2</sub>O<sub>8</sub> solution. After it was washed by deionized water, the PMMA/graphene film was dried in air. Subsequently, the film was placed onto Al<sub>2</sub>O<sub>3</sub> substrate and baked at 150 °C for 10 min to make good adhesion between graphene and the substrate. Finally, the PMMA is removed by acetone.

**MBE Growth:** GaN films were grown on the graphene-coated sapphire substrates through a plasma assisted molecular beam epitaxy (PA-MBE) system. Prior to GaN growth, the substrate was thermally degassed under ultrahigh vacuum at 500 °C for 30 min. Then, the wafer was kept at 500 °C and atomic nitrogen irradiation is performed with a

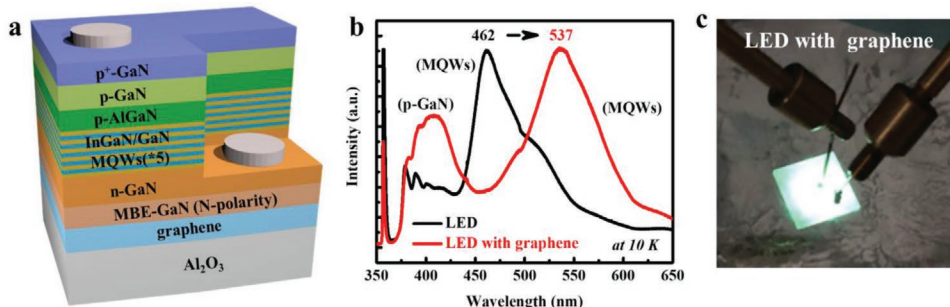


**Figure 6.** a) Schematic illustration of the InGaN-based LED structure grown on MBE-grown N-polarity GaN/graphene/Al<sub>2</sub>O<sub>3</sub> template. b) Low-temperature PL spectra of the InGaN-based LED structures grown on GaN/Al<sub>2</sub>O<sub>3</sub> template with or without atomic nitrogen irradiated graphene, showing the obviously red-shift of emission wavelength due to the polarity modulation related to graphene interlayer. c) Room temperature EL image of this N-polarity InGaN-based LED structure on GaN/Al<sub>2</sub>O<sub>3</sub> template with atomic nitrogen irradiated graphene.

nitrogen flow rate of 0.8 standard cubic centimeters per minute (sccm) and a radio frequency plasma forward power of 350 W. Then, the high temperature GaN layer was grown at 780 °C under slightly Ga-rich growth condition. The growth rate of GaN film is 3 nm min<sup>-1</sup>.

**MOVPE Growth:** InGaN/GaN green light-emitting diode (LED) structures were grown on the MBE-grown 800 nm-thickness GaN/sapphire templates with or without graphene interlayer by an AIXTRON 3 × 2 in. close-coupled showerhead reactor. H<sub>2</sub> was used as the carrier gas for the epitaxial process. The LED structure consists of a Si-doped GaN layer (2 μm), five periods of InGaN/GaN multiple-quantum-wells, a Mg-doped AlGaIn electron blocking layer (20 nm), a Mg-doped GaN layer (200 nm), and a heavy Mg-doped cap layer (10 nm). Each period of the MQW structure consists of a 15 nm-thick GaN barrier layer and a 2.5 nm-thick InGaIn well.

**Characterization:** XRD measurement was performed by X'Pert<sup>3</sup> MRD system using Cu Kα<sub>1</sub> X-ray source. Surface morphology was measured by scanning electron microscopy and atomic force microscopy (AFM) in tapping mode (Bruker Dimension ICON-PT). X-ray photoelectron spectroscopy (XPS) was performed to quantitatively estimate chemical composition of graphene before and after atomic nitrogen irradiation. The binding energies of the spectra were referred to that of the C 1s peak at 284.8 eV. Transmission electron microscopy characterization was performed by FEI Titan Cubed Themis G2 300. The photoluminescence of these LED structures were measured at 10 K under an excitation by a He–Cd laser with a pumping power of 30 mW and an excitation wavelength of 325 nm.

## Supporting Information

Supporting Information is available from the Wiley Online Library or from the author.

## Acknowledgements

F.L. and Z.Z. contributed equally to this work. This work was partly supported by the National Key R&D Program of China (No. 2017YFE0100300), Beijing Outstanding Young Scientist Program (No. BJJWZYJH0120191000103), the Science Challenge Project (No. TZ2016003), the National Natural Science Foundation of China (Nos. 61734001, 61521004, 61674010, and 61674068), Bureau of Industry and Information Technology of Shenzhen (No. 201901161512), and Beijing Natural Science Foundation (JQ19004).

## Conflict of Interest

The authors declare no conflict of interest.

## Keywords

graphene, III-nitrides, light emitting diodes, nitrogen lattice polarity, nucleation

Received: February 11, 2020

Revised: February 25, 2020

Published online:

[1] K. Chung, C. H. Lee, G. C. Yi, *Science* **2010**, 330, 655.

[2] C. H. Lee, Y. J. Kim, Y. J. Hong, S. R. Jeon, S. Bae, B. H. Hong, G. C. Yi, *Adv. Mater.* **2011**, 23, 4614.

[3] H. Yoo, K. Chung, Y. S. Choi, C. S. Kang, K. H. Oh, M. Kim, G. C. Yi, *Adv. Mater.* **2012**, 24, 515.

- [4] P. Gupta, A. A. Rahman, N. Hatui, J. B. Parmar, B. A. Chalke, R. D. Bapat, S. C. Purandare, M. M. Deshmukh, A. Bhattacharya, *Appl. Phys. Lett.* **2013**, 103, 181108.
- [5] S. Feng, B. Dong, Y. Lu, L. Yin, B. Wei, J. Wang, S. Lin, *Nano Energy* **2019**, 60, 836.
- [6] Z. Wu, Y. Lu, W. Xu, Y. Zhang, J. Li, S. Lin, *Nano Energy* **2016**, 30, 362.
- [7] K. Chung, H. Yoo, J. K. Hyun, H. Oh, Y. Tchoe, K. Lee, H. Baek, M. Kim, G. C. Yi, *Adv. Mater.* **2016**, 28, 7688.
- [8] J. B. Park, N. J. Kim, Y. J. Kim, S. H. Lee, G. C. Yi, *Curr. Appl. Phys.* **2014**, 14, 1437.
- [9] H. Ci, H. Chang, R. Wang, T. Wei, Y. Wang, Z. Chen, Y. Sun, Z. Dou, Z. Liu, J. Li, P. Gao, Z. Liu, *Adv. Mater.* **2019**, 31, 1901624.
- [10] Y. Qi, Y. Wang, Z. Pang, Z. Dou, T. Wei, P. Gao, S. Zhang, X. Xu, Z. Chang, B. Deng, S. Chen, Z. Chen, H. Ci, R. Wang, F. Zhao, J. Yan, X. Yi, K. Liu, H. Peng, Z. Liu, L. Tong, J. Zhang, Y. Wei, J. Li, Z. Liu, *J. Am. Chem. Soc.* **2018**, 140, 11935.
- [11] Q. Wu, J. Yan, L. Zhang, X. Chen, T. Wei, Y. Li, Z. Liu, X. Wei, Y. Zhang, J. Wang, J. Li, *CrystEngComm* **2017**, 19, 5849.
- [12] Y. Kobayashi, K. Kumakura, T. Akasaka, *Nature* **2012**, 484, 223.
- [13] J. Kim, C. Bayram, H. Park, C. W. Cheng, C. Dimitrakopoulos, J. A. Ott, K. B. Reuter, S. W. Bedell, D. K. Sadana, *Nat. Commun.* **2014**, 5, 4836.
- [14] T. Ayari, S. Sundaram, X. Li, Y. E. Gmili, P. L. Voss, J. P. Salvestrini, A. Ougazzaden, *Appl. Phys. Lett.* **2016**, 108, 171106.
- [15] T. H. Seo, A. H. Park, S. Park, Y. H. Kim, G. H. Lee, M. J. Kim, M. S. Jeong, Y. H. Lee, Y. B. Hahn, E. K. Suh, *Sci. Rep.* **2015**, 5, 7747.
- [16] M. Heilmann, G. Sarau, M. Göbel, M. Latzel, S. Sadhujan, C. Tessarek, S. Christiansen, *Cryst. Growth Des.* **2015**, 15, 2079.
- [17] Z. Chen, X. Zhang, Z. Dou, T. Wei, Z. Liu, Y. Qi, H. Ci, Y. Wang, Y. Li, H. Chang, J. Yan, S. Yang, Y. Zhang, J. Wang, P. Gao, J. Li, Z. Liu, *Adv. Mater.* **2018**, 30, 1801608.
- [18] J. K. Choi, J. H. Huh, S. D. Kim, D. Moon, D. Yoon, K. Joo, J. Kwak, J. H. Chu, S. Y. Kim, K. Park, Y. W. Kim, E. Yoon, H. Cheong, S. Y. Kwon, *Nanotechnology* **2012**, 23, 435603.
- [19] T. Li, C. Liu, Z. Zhang, B. Yu, H. Dong, W. Jia, Z. Jia, C. Yu, L. Gan, B. Xu, *AIP Adv.* **2018**, 8, 045105.
- [20] S. J. Chae, Y. H. Kim, T. H. Seo, D. L. Duong, S. M. Lee, M. H. Park, E. S. Kim, J. J. Bae, S. Y. Lee, H. Jeong, E. K. Suh, C. W. Yang, M. S. Jeong, Y. H. Lee, *RSC Adv.* **2015**, 5, 1343.
- [21] K. Chung, S. I. Park, H. Baek, J. S. Chung, G. C. Yi, *NPG Asia Mater.* **2012**, 4, e24.
- [22] H. Chang, Z. Chen, W. Li, J. Yan, R. Hou, S. Yang, Z. Liu, G. Yuan, J. Wang, J. Li, P. Gao, T. Wei, *Appl. Phys. Lett.* **2019**, 114, 091107.
- [23] Q. Zeng, Z. Chen, Y. Zhao, T. Wei, X. Chen, Y. Zhang, G. Yuan, J. Li, *Jpn. J. Appl. Phys.* **2016**, 55, 085501.
- [24] A. Kovács, M. Duchamp, R. E. Dunin-Borkowski, R. Yakimova, P. L. Neumann, H. Behmenburg, B. Foltynski, C. Giesen, M. Heuken, B. Pécz, *Adv. Mater. Interfaces* **2015**, 2, 1400230.
- [25] N. Nepal, V. D. Wheeler, T. J. Anderson, F. J. Kub, M. A. Mastro, R. L. Myers-Ward, S. B. Qadri, J. A. Freitas, S. C. Hernandez, L. O. Nyakiti, S. G. Walton, K. Gaskill, C. R. Eddy Jr., *Appl. Phys. Express* **2013**, 6, 061003.
- [26] Y. Xu, B. Cao, Z. Li, D. Cai, Y. Zhang, G. Ren, J. Wang, L. Shi, C. Wang, K. Xu, *ACS Appl. Mater. Interfaces* **2017**, 9, 44001.
- [27] K. Chung, H. Beak, Y. Tchoe, H. Oh, H. Yoo, M. Kim, G. C. Yi, *APL Mater.* **2014**, 2, 092512.
- [28] Y. Li, Y. Zhao, T. Wei, Z. Liu, R. Duan, Y. Wang, X. Zhang, Q. Wu, J. Yan, X. Yi, G. Yuan, J. Wang, J. Li, *Jpn. J. Appl. Phys.* **2017**, 56, 085506.
- [29] J. W. Shon, J. Ohta, K. Ueno, A. Kobayashi, H. Fujioka, *Sci. Rep.* **2015**, 4, 5325.
- [30] Y. L. Wang, F. Ren, U. Zhang, Q. Sun, C. D. Yerino, T. S. Ko, Y. S. Cho, I. H. Lee, J. Han, S. J. Pearton, *Appl. Phys. Lett.* **2009**, 94, 212108.

- [31] A. Das, A. Das, L. B. Chang, C. S. Lai, R. M. Lin, F. C. Chu, Y. H. Lin, L. Chow, M. J. Jeng, *Appl. Phys. Express* **2013**, *6*, 036601.
- [32] F. Akyol, D. N. Nath, S. Krishnamoorthy, P. S. Park, S. Rajan, *Appl. Phys. Lett.* **2012**, *100*, 111118.
- [33] K. Shojiki, T. Tanikawa, J. H. Choi, S. Kuboya, T. Hanada, R. Katayama, T. Matsuoka, *Appl. Phys. Express* **2015**, *8*, 061005.
- [34] X. Xu, Z. Zhang, J. Dong, D. Yi, J. Niu, M. Wu, L. Lin, R. Yin, M. Li, J. Zhou, S. Wang, J. Sun, X. Duan, P. Gao, Y. Jiang, X. Wu, H. Peng, R. S. Ruoff, Z. Liu, D. Yu, E. Wang, F. Ding, K. Liu, *Sci. Bull.* **2017**, *62*, 1074.
- [35] A. R. Smith, R. M. Feenstra, D. W. Greve, J. Neugebauer, J. E. Northrup, *Phys. Rev. Lett.* **1997**, *79*, 3934.
- [36] F. S. Tautz, S. Sloboshanin, U. Starke, J. A. Schaefer, *J. Phys.: Condens. Matter* **1999**, *11*, 8035.
- [37] K. Xu, N. Yano, A. W. Jia, A. Yoshikawa, K. Takahashi, *J. Cryst. Growth* **2002**, *237-239*, 1003.
- [38] Y. Feng, X. Yang, Z. Zhang, D. Kang, J. Zhang, K. Liu, X. Li, J. Shen, F. Liu, T. Wang, P. Ji, F. Xu, N. Tang, T. Yu, X. Wang, D. Yu, W. Ge, B. Shen, *Adv. Funct. Mater.* **2019**, *29*, 1905056.